A key requirement for synaptic Reelin signaling in ketamine-mediated behavioral and synaptic action

Ji-Woon Kim[a,b,c], Joachim Herz[c,d,e], Ege T. Kavalali[a,b,c], and Lisa M. Monteggia[a,b,c,1]

[a]Department of Pharmacology, Vanderbilt University, Nashville, TN 37240-7933; [b]Vanderbilt Brain Institute, Vanderbilt University, Nashville, TN 37240-7933; [c]Department of Neuroscience, The University of Texas Southwestern Medical Center, Dallas, TX 75390-9111; [d]Department of Molecular Genetics, The University of Texas Southwestern Medical Center, Dallas, TX 75390; and [e]Department of Neurology and Neurotherapeutics, The University of Texas Southwestern Medical Center, Dallas, TX 75390

Ketamine is a noncompetitive *N*-methyl-D-aspartate (NMDA) receptor antagonist that produces rapid antidepressant action in some patients with treatment-resistant depression. However, recent data suggest that ~50% of patients with treatment-resistant depression do not respond to ketamine. The factors that contribute to the nonresponsiveness to ketamine's antidepressant action remain unclear. Recent studies have reported a role for secreted glycoprotein Reelin in regulating pre- and postsynaptic function, which suggests that Reelin may be involved in ketamine's antidepressant action, although the premise has not been tested. Here, we investigated whether the disruption of Reelin-mediated synaptic signaling alters ketamine-triggered synaptic plasticity and behavioral effects. To this end, we used mouse models with genetic deletion of Reelin or apolipoprotein E receptor 2 (Apoer2), as well as pharmacological inhibition of their downstream effectors, Src family kinases (SFKs) or phosphoinositide 3-kinase. We found that disruption of Reelin, Apoer2, or SFKs blocks ketamine-driven behavioral changes and synaptic plasticity in the hippocampal CA1 region. Although ketamine administration did not affect tyrosine phosphorylation of DAB1, an adaptor protein linked to downstream signaling of Reelin, disruption of Apoer2 or SFKs impaired baseline NMDA receptor–mediated neurotransmission. These results suggest that maintenance of baseline NMDA receptor function by Reelin signaling may be a key permissive factor required for ketamine's antidepressant effects. Taken together, our results suggest that impairments in Reelin-Apoer2-SFK pathway components may in part underlie nonresponsiveness to ketamine's antidepressant action.

ketamine | antidepressant | Reelin | Apoer2 | NMDA receptor

Major depressive disorder (MDD) is a serious disorder that affects ~20.6% of the US population and is a leading cause of suicide (1). One crucial problem in treating patients with MDD is an incomplete response rate to medications, where a large fraction of patients do not show a response to primary antidepressant medications (2, 3). Recent clinical findings demonstrate that a subanesthetic dose of ketamine, a noncompetitive *N*-methyl-D-aspartate receptor (NMDAR) antagonist, produces rapid antidepressant effects within hours in some patients with treatment-resistant depression or MDD (4–6). However, ~50% of patients with treatment-resistant depression do not respond to ketamine (7), and factors involved in the nonresponsiveness to ketamine remain unclear.

The hippocampus is a brain region that has been linked to the pathophysiological changes in MDD. Patients with MDD show a decrease in hippocampal volume and function (8–12). In contrast, MDD patients treated with classic antidepressants have a reversal in hippocampal volume changes along with an improvement in hippocampus-dependent cognitive function (13–15). Previous preclinical studies have shown animal models of depression also exhibit a decrease in hippocampal volume and function (13), and hippocampal synaptic functional enhancement is required to mediate antidepressant responses (16–18). This enhancement of hippocampal function has been suggested to be a key requirement to exert an antidepressant response.

Ketamine induces rapid molecular changes that elicit synaptic plasticity in the hippocampus (16, 19–22). Specifically, ketamine rapidly generates synaptic potentiation of field excitatory postsynaptic potentials (fEPSPs) in CA3–CA1 synapses in the hippocampus (ketamine potentiation) by inducing the rapid translation of brain-derived neurotrophic factor (BDNF) and trafficking of α-amino-3-hydroxy-5-methyl-4-isoxazolepropionic acid receptors (AMPARs) onto the postsynaptic surface (16, 19, 23, 24). Recent studies have shown that if key factors for the antidepressant effects of ketamine, such as BDNF (16, 25, 26) or AMPA receptors (16, 27), are deleted or blocked, the synaptic potentiation in the hippocampus concurrently disappears, suggesting that the synaptic potentiation underlies ketamine's antidepressant effects (16, 19).

Ketamine-mediated potentiation of fEPSPs in CA3–CA1 synapses has been shown to require a block of NMDAR activation by spontaneous glutamate release. Ketamine produces synaptic potentiation in the presence of tetrodotoxin, which blocks sodium channels, and thereby the generation of action potentials, suggesting that blocking NMDARs activated by the spontaneous presynaptic release is key to producing the synaptic potentiation (19, 21, 28, 29). In agreement with this premise, deletion of Vps10p-tail-interactor-1a (Vti1a) and vesicle-associated membrane protein 7 (VAMP7), which are soluble *N*-ethylmaleimide–sensitive factor attachment protein receptor proteins selectively involved in spontaneous neurotransmitter release (30, 31) in the CA3 hippocampal region, occluded the ketamine potentiation (32). Collectively, these lines of evidence suggest spontaneous glutamate release, and NMDARs are important factors for ketamine potentiation.

Significance

Ketamine exerts rapid antidepressant action in some patients with treatment-resistant depression. This study demonstrates that Reelin, its receptor apolipoprotein E receptor 2 (Apoer2), and downstream signaling via Src family kinases are required for ketamine-mediated behavioral changes and associated synaptic plasticity in the CA1 hippocampal region. Our findings suggest that a permissive role of Reelin-dependent synaptic signaling in regulating the basal activity of N-methyl-D-aspartate receptors may be essential for ketamine's antidepressant efficacy.

NEUROSCIENCE

Thus, it is possible that if these pre- or postsynaptic components are impaired, ketamine may not produce the synaptic potentiation and antidepressant effects.

Reelin is a secreted glycoprotein and acts as a neuromodulator in the adult brain by regulating pre- and postsynaptic machinery. Reelin binds to its receptors, apolipoprotein E receptor 2 (Apoer2) and very-low-density lipoprotein receptor (VLDLR) and increases tyrosine phosphorylation in Disabled-1 (DAB1) (33–35). The Reelin pathway regulates pre- or postsynaptic function through its downstream signaling pathways in the adult brain. In presynaptic terminals, the Reelin-Apoer2 pathway activates phosphoinositide 3-kinase (PI3K) and increases Ca^{2+} release from intracellular stores, which in turn mobilizes VAMP7-containing synaptic vesicles and augments spontaneous release (31). At the postsynaptic sites, Reelin's binding to Apoer2 reciprocally activates DAB1 and Src family kinases (SFKs). Subsequently, the activated SFKs increase tyrosine phosphorylation in NMDAR subunits, GluN2A and GluN2B (34–37), and increase NMDAR open probability (37–39). Since pre- and postsynaptic components regulated by Reelin have been suggested to be important for ketamine potentiation (16, 19–21, 32), it is conceivable that disrupted Reelin signaling may abrogate the antidepressant action and synaptic plasticity of ketamine.

To examine this premise, we used genetically modified mice with a deletion of either Reelin or Apoer2 and investigated changes in antidepressant-like behaviors and synaptic potentiation in the CA1 hippocampal region following ketamine treatment. We also used pharmacological inhibitors to examine the effects of signaling molecules downstream of Reelin-Apoer2, specifically SFKs and PI3K, on ketamine-induced behavioral changes and synaptic plasticity. Lastly, we investigated whether the disruption of ketamine's effects is due to a requirement for the activation of Reelin-dependent signaling or the impairment of NMDAR function by the disruption of Reelin-dependent signaling. Our results suggest that disruption of the Reelin-Apoer2-SFKs pathway depresses NMDAR function and diminishes ketamine's use-dependent NMDAR antagonism, thereby rendering synapses nonresponsive to ketamine's action as well as subsequent antidepressant responses. Taken together, these results provide insight into understanding the cellular and molecular mechanisms underlying ketamine's antidepressant effects.

Results

Genetic Deletion of Reelin in the Adult Brain Abolishes the Ketamine-Mediated Behavioral Changes and Synaptic Potentiation. To investigate the effects of disrupted Reelin on the ketamine-mediated behavioral and synaptic changes, we generated conditional knockout (cKO) mice by mating Reelin^flox/flox mice with an inducible Cre-expressing line (CAG-CreERT2) using tamoxifen treatment, as previously reported (40). Since Reelin is important in the development of the brain structure (41), tamoxifen was given at 2 mo of age to delete Reelin after the developmental period and thereby avoid potential confounding factors. In this cKO mouse, Reelin expression is decreased to less than 5% in the hippocampal region and globally in the brain after tamoxifen treatment. There were no developmental defects in the cKO mice, as previously described (40).

The forced swim test (FST) has been shown to have high predictive and face validity for ketamine-mediated antidepressant action (16, 25–27, 42). Therefore, we examined the rapid, antidepressant-like effects of ketamine 2 h after injection in Reelin cKO and wild-type (WT) littermate control mice in the FST. Ketamine treatment significantly reduced the time spent immobile in the WT but not Reelin cKO mice (Fig. 1A). We also observed that ketamine treatment increased the swimming time of WT mice but not Reelin cKO mice (SI Appendix, Fig. S1A). Together, these results suggest Reelin is necessary for the ketamine-mediated behavioral changes in the FST.

We next investigated the effects of Reelin on ketamine-induced hippocampal synaptic plasticity. fEPSPs were measured before and after ketamine or vehicle (artificial cerebrospinal fluid, ACSF) application in the CA1 hippocampal area of Reelin WT and cKO mice. Ketamine application produced significant synaptic potentiation in WT slices but not in cKO slices, compared with slices perfused with ACSF under the same conditions (Fig. 1 B and C). We also analyzed the input–output (I–O) relationship before and after ketamine treatment to validate the changes in basal neurotransmission. The slope change ratio of the I–O curve was significantly increased after ketamine treatment in WT but not cKO slices (Fig. 1 D and E), indicating a requirement of Reelin for ketamine-enhanced synaptic efficacy. The comparison of slopes of I–O curves between WT and cKO slices during baseline recordings revealed no significant difference (SI Appendix, Fig. S2A), suggesting that the abolished ketamine effects are not due to impaired basal neurotransmission. We also analyzed paired-pulse ratios (PPRs) in the WT and cKO slices to determine if any presynaptic functional changes were induced by ketamine treatment or genotype factor. No significant changes were observed in all comparison groups, suggesting that presynaptic release probability was not affected by ketamine or deletion of Reelin (SI Appendix, Fig. S3 A–C).

Genetic Deletion of Apoer2 Blocks the Behavioral Changes and Synaptic Potentiation by Ketamine. Reelin activates downstream signaling by binding to its receptors, Apoer2 and VLDLR (33, 35, 36, 43, 44). We, therefore, considered the downstream signaling of Reelin through Apoer2 or VLDLR in ketamine-mediated behavioral and synaptic changes. Previous studies have demonstrated that Reelin has a six to nine times higher binding affinity for Apoer2 than the VLDLR, indicating a more crucial role of Apoer2 in Reelin-dependent signaling, compared with the VLDLR in physiological conditions (36, 45, 46). In addition, Vldlr knockout (KO) mice have confounding factors for behavioral analysis, such as a hyperactivity phenotype, that is not observed in Apoer2 KO mice (36). Therefore, we investigated ketamine-mediated behavioral and synaptic changes in Apoer2 KO mice.

We tested the Apoer2 KO mice and WT littermate controls in the FST. Ketamine-treated WT littermate control mice showed a significant reduction in the time spent immobile compared with vehicle-treated WT mice. Unexpectedly, saline-treated Apoer2 KO mice also showed a significant reduction of immobility compared with saline-treated WT mice, indicating that the deletion of Apoer2 reduces the baseline in the FST. However, ketamine treatment did not further reduce the duration of immobility in Apoer2 KO mice compared with saline-treated Apoer2 KO mice (Fig. 2A). Conversely, in the measurement of cumulative swimming duration, Apoer2 KO mice showed an increase in swimming duration compared with saline-treated WT mice, and ketamine treatment did not further increase the swimming duration in Apoer2 KO mice (SI Appendix, Fig. S1B). These data suggest that the deletion of Apoer2 occludes ketamine-mediated behavioral effects in the FST. To confirm the occluded antidepressant-like effects of ketamine in Apoer2 KO mice, we next performed the novelty-suppressed feeding test (NSFT) and evaluated anhedonia-like behaviors by measuring the latency to feed (47). Ketamine significantly reduced the latency to feed in WT mice compared with vehicle-treated WT mice, indicative of an antidepressant-like effect of ketamine. Unlike the baseline change in the FST, vehicle-treated Apoer2 KO mice did not show any significant change in the latency to feed compared with vehicle-treated WT mice. However, ketamine did not change the latency to feed in Apoer2 KO mice (Fig. 2B). To confirm that the results of NSFT are not induced by abnormal food intake, we measured the weight of consumed chow immediately after the NSFT. No significant difference was observed between groups (Fig. 2C). Taken together, these results
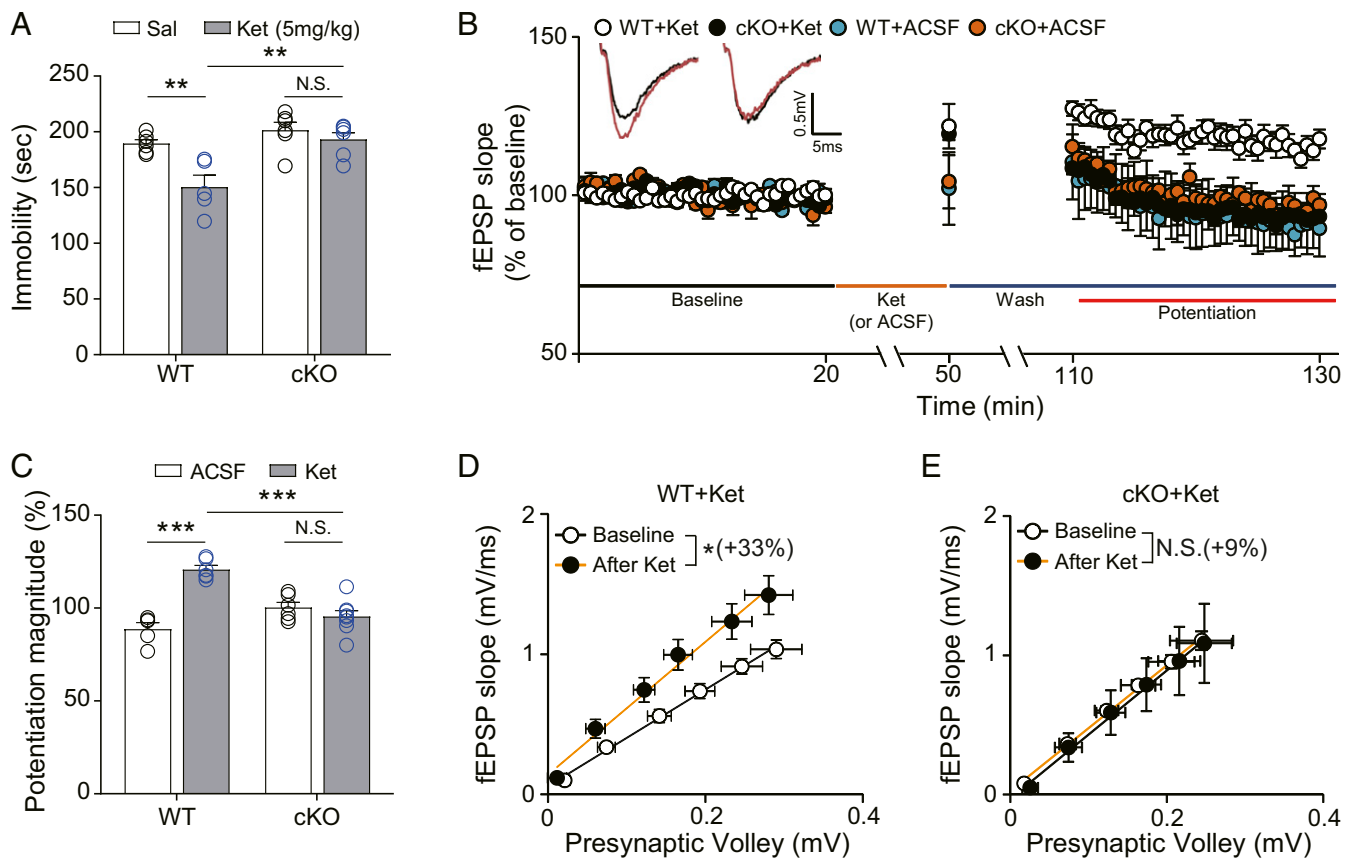
Fig. 1. Ketamine does not produce antidepressant-like behavioral changes and synaptic potentiation in *Reelin* cKO mice. (*A*) Accumulated time mice spent immobile during the FST performed 2 h after ketamine injection. Ketamine significantly decreased immobility in WT mice but not in cKO mice [two-way ANOVA with Tukey's multiple comparisons, Genotype × Drug: $F_{(1, 19)} = 4.815$, $P = 0.0408$, Genotype: $F_{(1, 19)} = 15.68$, $P = 0.0008$, Drug: $F_{(1, 19)} = 11.47$, $P = 0.0031$, $n = 5$ to 6 per group]. (*B*) Ketamine potentiation was measured after 20 min of baseline measurement, 30 min of ketamine perfusion, and 1 h of washout period in the hippocampal CA1 region. All responses were normalized to respective baselines. (*Inset*) Representative waveforms from baseline (black) or ketamine potentiation (red) measurement. (*C*) A bar graph that summarizes the magnitude of ketamine potentiation of respective groups measured in *B*. Significantly increased potentiation magnitude by ketamine was observed in WT mice but not in cKO mice [two-way ANOVA with Tukey's multiple comparisons, Genotype × Drug: $F_{(1, 21)} = 37.82$, $P < 0.0001$, Genotype: $F_{(1, 21)} = 5.226$, $P = 0.0327$, Drug: $F_{(1, 21)} = 20.50$, $P = 0.0002$, $n = 5$ to 8 per group]. (*D* and *E*) I–O curves measured during baseline and potentiation measurement in *B*. Initial slopes of fEPSPs versus presynaptic volley values are plotted at 4, 8, 12, 16, 20, and 24 μA stimulation intensity. The slope of the I–O curve is significantly increased after ketamine treatment in slices from WT mice but not in slices from cKO mice [paired *t* test, WT+Ket (*D*): $t_{(5)} = 3.671$, $P = 0.0144$, $n = 6$; cKO+Ket (*E*): $t_{(7)} = 1.129$, $P = 0.2961$, $n = 8$]. All data represented as mean ± SEM; *$P < 0.05$, **$P < 0.01$, and ***$P < 0.001$.

suggest that the deletion of *Apoer2* occludes or abolishes ketamine-mediated, antidepressant-like behavioral changes.

Next, to examine whether the ketamine potentiation is affected by the *Apoer2* deletion, we measured fEPSPs in CA1 hippocampal slices collected from *Apoer2* WT or KO mice. In WT slices, ketamine treatment produced a significant potentiation that was not observed in the KO slices (Fig. 2 *D* and *E*). In the analysis of the I–O curve before and after the ketamine treatment, the slope of the I–O curve was significantly increased after ketamine treatment in both the WT slices and the KO slices (Fig. 2 *F* and *G*). However, ketamine perfusion increased the slope of the I–O curve to 62% in the WT slices (WT+Ket in Fig. 2*F*) but only to 14% in the KO slices (KO+Ket in Fig. 2*G*), showing attenuation of ketamine-mediated synaptic changes in *Apoer2* KOs. In the comparison of the baseline I–O curve between the WT and *Apoer2* KO slices, there was no significant difference (*SI Appendix*, Fig. S2*B*), suggesting that the deletion of *Apoer2* does not affect basal neurotransmission. We also examined PPRs by ketamine treatment or genotype factor in the WT and KO slices. No significant changes were observed in any of the comparison groups (*SI Appendix*, Fig. S3 *D–F*), indicating that presynaptic release is not changed by ketamine or the deletion of *Apoer2*.

Pharmacological Inhibition of Src Family Kinases Blocks the Behavioral Effects and Synaptic Potentiation by Ketamine. Our results show that the deletion of *Reelin* and its receptor, *Apoer2*, blocked the antidepressant-like behavioral effects and synaptic functional changes following ketamine treatment. These results suggest that signaling molecules downstream of Reelin-Apoer2 may be involved in ketamine's antidepressant efficacy. One possible signaling pathway is an SFKs-dependent postsynaptic pathway. SFKs, such as Src and Fyn, are nonreceptor tyrosine kinases that increase tyrosine phosphorylation of NMDAR subunits (GluN2A and GluN2B) in response to Reelin (35, 37). These phosphorylation changes activate NMDAR function, increase Ca^{2+} influx through the NMDAR (37–39), and also counter the beta-amyloid–mediated decrease in NMDAR function (48). Since ketamine is an open-channel NMDAR blocker that acts in a use-dependent manner (49), inhibition of SFKs may impair ketamine's NMDAR blockade by suppressing the opening of the NMDAR channel (38, 50). To test this hypothesis, we used a brain-penetrable, SFKs-specific inhibitor, AZD0530 (AZD) (51, 52). To validate its pharmacological action, we measured the phosphorylation level of GluN2A (Y1325) and GluN2B (Y1472), known target residues for SFKs (53, 54), in the hippocampus 30 min after intraperitoneal (i.p.) injection of
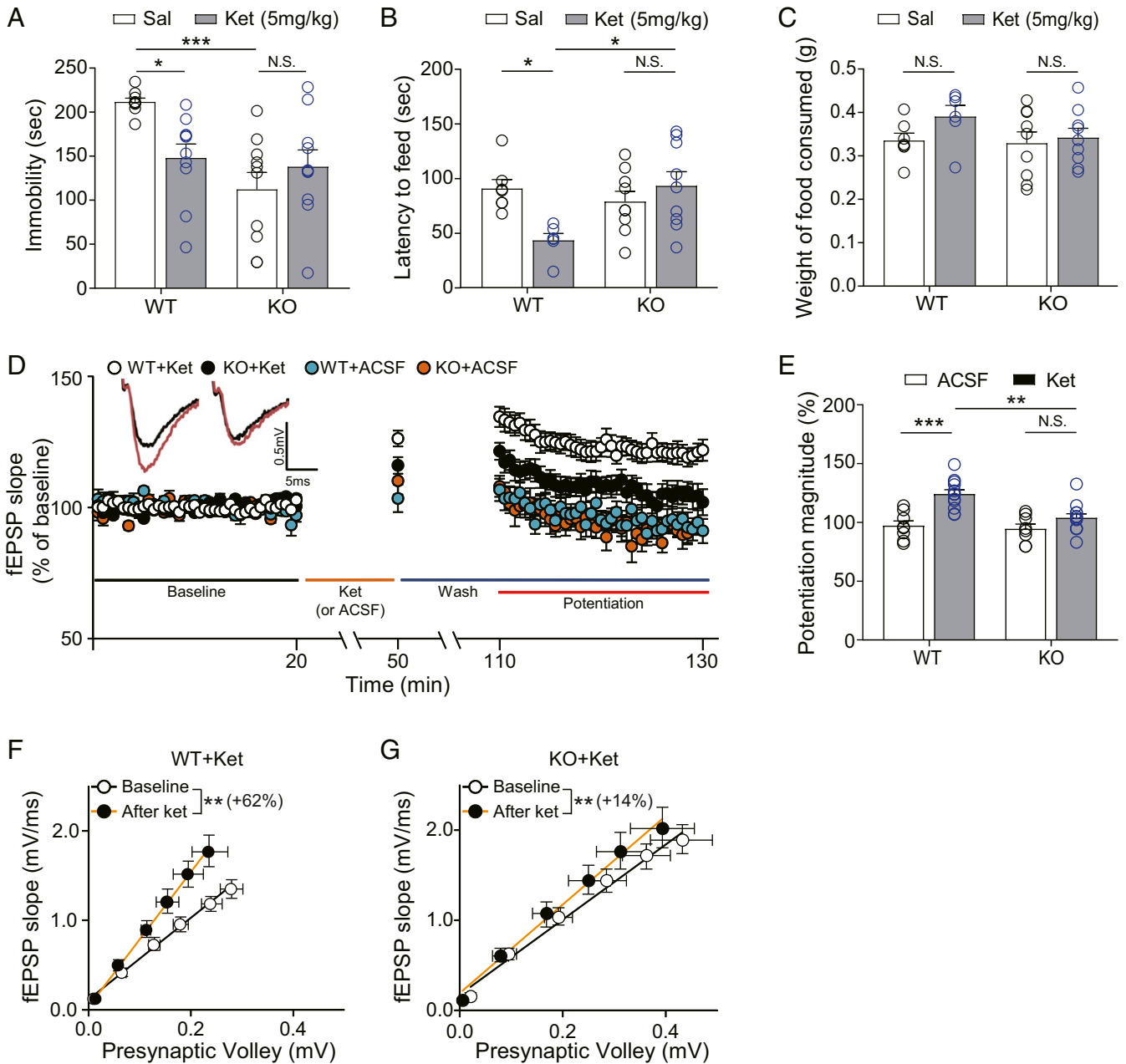
NEUROSCIENCE

Fig. 2. Ketamine does not produce antidepressant-like behavioral changes and synaptic potentiation in *Apoer2* KO mice. (*A*) Accumulated time mice spent immobile during the FST performed 2 h after ketamine injection. Ketamine significantly decreased immobility in WT mice. *Apoer2* KO mice showed reduced immobility, compared with vehicle-treated WT mice. Ketamine did not further reduce the immobility in *Apoer2* KO mice [two-way ANOVA with Tukey's multiple comparisons, Genotype × Drug: $F_{(1, 35)} = 7.535$, $P = 0.0095$, Genotype: $F_{(1, 35)} = 11.36$, $P = 0.0018$, Drug: $F_{(1, 35)} = 1.362$, $P = 0.2511$, $n = 9$ to 10 mice per group]. (*B*) NSFT. Latency to feed was measured 2 h after ketamine i.p. injection. Ketamine significantly reduced latency to feed in WT mice but not in *Apoer2* KO mice [two-way ANOVA with Tukey's multiple comparisons, Genotype × Drug: $F_{(1, 27)} = 8.509$, $P = 0.0070$, Genotype: $F_{(1, 27)} = 3.194$, $P = 0.0851$, Drug: $F_{(1, 27)} = 2.413$, $P = 0.1319$, $n = 6$ to 9 per group]. (*C*) A bar graph that represents the amount of consumed food. Immediately after the NSFT, the mouse was transferred to the home cage and the amount of food consumed for 5 min was measured. No statistical significance was observed in any comparisons between groups [two-way ANOVA with Tukey's multiple comparisons, Genotype × Drug: $F_{(1, 27)} = 0.803$, $P = 0.3782$, Genotype: $F_{(1, 27)} = 1.352$, $P = 0.2551$, Drug: $F_{(1, 27)} = 2.087$, $P = 0.1591$, $n = 6$ to 9 per group]. (*D*) Ketamine potentiation was measured after 20 min of baseline measurement, 30 min of ketamine perfusion, and 1 h of washout period in the hippocampal CA1 region. All responses were normalized to respective baselines. (*Inset*) Representative waveforms during baseline (black) or ketamine potentiation (red) measurement. (*E*) A bar graph that summarizes the magnitude of ketamine potentiation of respective groups measured in *D*. Significantly increased potentiation magnitude by ketamine was observed in WT mice but not in KO mice [two-way ANOVA with Tukey's multiple comparisons, Genotype × Drug: $F_{(1, 36)} = 5.181$, $P = 0.0289$, Genotype: $F_{(1, 36)} = 8.669$, $P = 0.0056$, Drug: $F_{(1, 36)} = 21.62$, $P < 0.0001$, $n = 8$ to 12 per group]. (*F* and *G*) I–O curves measured during baseline and potentiation measurement in *D*. Initial slopes of fEPSPs versus presynaptic volley values are plotted at 4, 8, 12, 16, 20, and 24 μA stimulation intensity. The slope of the I–O curve was significantly increased after ketamine treatment in both the WT slices and the KO slices [paired *t* test, WT+Ket (*F*): $t_{(9)} = 3.334$, $P = 0.0087$, $n = 10$; KO+Ket (*G*): $t_{(10)} = 3.709$, $P = 0.004$, $n = 11$]. However, the increase rate of the slope by ketamine perfusion was 62% in the WT+Ket group but only 14% in the KO+Ket group. All data represented as mean ± SEM; *$P < 0.05$, **$P < 0.01$, and ***$P < 0.001$.

Kim et al.
A key requirement for synaptic Reelin signaling in ketamine-mediated behavioral and synaptic action

AZD. The AZD treatment resulted in a significant decrease in phosphorylation of GluN2A and a slight but not significant decrease in phosphorylation of GluN2B compared with the respective vehicle-treated groups (Fig. 3A). These results show that an i.p. injection of AZD inhibits SFKs in the hippocampus, although the inhibition was not strong enough to decrease the phosphorylation level of GluN2B. Next, we conducted the FST, with mice given AZD 30 min before ketamine injection and tested 2 h after the ketamine injection. We found that AZD-pretreated mice did not show changes in the duration of immobility or swimming following ketamine treatment (Fig. 3B and *SI Appendix*, Fig. S1C), suggesting that inhibition of SFKs prevents ketamine-mediated behavioral changes in the FST.

Next, we investigated the effects of SFK inhibition on ketamine potentiation with PP2, a widely used SKF inhibitor. We treated slices with PP2 during the entire recording and measured ketamine potentiation. Ketamine treatment produced a significant potentiation in vehicle-treated slices but not in PP2-pretreated slices (Fig. 3 C and D). We confirmed that inhibition of SFKs attenuated ketamine potentiation by also examining AZD. Similar to PP2, AZD application significantly reduced ketamine potentiation (*SI Appendix*, Fig. S4). We next analyzed the slope of the I–O curve before and after ketamine treatment and observed that the slope of the I–O curve was markedly increased by ketamine treatment in both the vehicle-treated slices and the PP2-treated slices. However, ketamine perfusion showed a 66% increase in the slope of the I–O curve in the vehicle-treated slices (Veh+Ket in Fig. 3E) but only 15% in the PP2-treated slices (PP2+Ket in Fig. 3F). These results show that inhibition of SFKs impairs ketamine-mediated synaptic changes. The slopes of the I–O curves during baseline recording were not markedly different between vehicle- and PP2-treated slices (*SI Appendix*, Fig. S2C), suggesting that the inhibition of SFKs does not affect basal neurotransmission. We also observed that neither ketamine nor PP2 treatment altered PPRs (*SI Appendix*, Fig. S3 G–I), indicating that presynaptic release is not affected either by ketamine or SFKs inhibition. Lastly, to confirm the pharmacological blockade by PP2 during the recordings, we measured tyrosine phosphorylation levels of GluN2A and GluN2B, which are both SFK substrates, in recorded slices. The phosphorylation levels of GluN2A and GluN2B were significantly reduced in the PP2-treated slices compared with the vehicle-treated slices (Fig. 3G), demonstrating that the abolished ketamine potentiation by PP2 treatment is possibly due to suppression of NMDAR phosphorylation and activity (37–39, 55).

Pharmacological Inhibition of PI3K Does Not Block Ketamine Potentiation. The results presented show that Reelin's control of postsynaptic signaling impacts ketamine's action. Next, we examined the role of Reelin in presynaptic signaling underlying spontaneous release. Reelin is known to increase spontaneous neurotransmission in presynaptic terminals through activation of the PI3K-AKT pathway (31). Since we previously showed that impaired spontaneous neurotransmission occludes ketamine potentiation (32), we examined the effects of PI3K inhibition on ketamine-induced synaptic potentiation with LY294002, a PI3K inhibitor. We found that ketamine treatment produced robust synaptic potentiation in vehicle-treated slices as well as in LY294002-treated slices (Fig. 4 A and B). Ketamine treatment also significantly increased the slope of the I–O curve in both vehicle- and LY294002-treated slices (Fig. 4 C and D), indicating that PI3K inhibition does not affect ketamine-induced augmentation of synaptic plasticity. The slopes of the I–O curves during baseline in both vehicle- and LY294002-treated slices were indistinguishable (*SI Appendix*, Fig. S2D). There were also no significant differences in PPRs by either ketamine or LY294002 treatment (*SI Appendix*, Fig. S3 J–L). These results suggest that PI3K inhibition does not affect basal pre- and postsynaptic function. To confirm the pharmacological effect of LY294002 under our study conditions, we measured the phosphorylation level of

AKT, a substrate of PI3K, in the recorded slices. In LY294022-treated slices, AKT phosphorylation was significantly reduced compared with vehicle-treated slices (Fig. 4E).

Disruption of Apoer2 or SFKs Suppresses NMDAR Function. Our results show that blocking Reelin, Apoer2, or SFKs signaling prevents the antidepressant-like behavioral changes and synaptic potentiation induced by ketamine. These results can be interpreted in two ways. First, activation of the Reelin-Apoer2-SFKs pathway may be required for the ketamine-mediated behavioral and synaptic changes. Or secondly, disruption of the Reelin-Apoer2-SFKs pathway may impair baseline NMDAR-mediated neurotransmission and thereby occlude the ketamine's effects. To examine these possibilities, we measured the expression of Reelin and the phosphorylation levels of GluN2A and GluN2B (Fig. 5 A and B), which are substrates of the Reelin-Apoer2-SFKs pathway (35), in the hippocampus 10 and 30 min after ketamine injection. We observed that the Reelin expression level was similar in the ketamine-treated group compared with the saline-treated group. However, the phosphorylation level of GluN2A was significantly increased 10 min after ketamine treatment, raising the possibility that ketamine may facilitate Reelin-dependent signaling. The increased phosphorylation level was normalized to baseline 30 min after injection (Fig. 5 A and B). In contrast, the phosphorylation level of GluN2B was not significantly changed at the 10 or 30 min time point (Fig. 5 A and B). We also examined the phosphorylation of AKT to confirm the effects of ketamine on the PI3K pathway. Consistent with the above finding that PI3K inhibition does not impact ketamine-induced synaptic plasticity, no significant changes in AKT phosphorylation were observed at any tested time points (Fig. 5 A and B).

Although Reelin protein expression and its downstream signaling effectors, such as GluN2B and AKT, were not significantly altered by ketamine, it is still possible that the increased secretion of Reelin may activate its downstream signaling and transiently increase phosphorylation of GluN2A. Previous studies have shown that phosphorylation at tyrosine residues of DAB1 is a key determinant of the activated Reelin-dependent signaling pathway (33–35). Thus, we examined the levels of DAB1 tyrosine phosphorylation with immunoprecipitation 10 min after ketamine injection to confirm whether the increased phospho-GluN2A level is due to activated Reelin signaling. However, the tyrosine phosphorylation levels of DAB1 in ketamine-treated mice were comparable to those of saline-treated mice, suggesting that the transient increase in GluN2A phosphorylation by ketamine is not induced by the activation of Reelin signaling (Fig. 5C).

Next, we tested the second possibility that disruption of the Reelin-Apoer2-SFKs pathway leads to the suppression of basal NMDAR function. Since ketamine is a use-dependent NMDAR antagonist (49), if the NMDAR function is suppressed by the disruption of Reelin-Apoer2-SFKs, then ketamine's action on the NMDAR would be expected to be attenuated. To explore this possibility, we measured NMDAR-induced fEPSPs from *Apoer2* KO mice or PP2-treated slices and analyzed I–O curves. The slopes of the NMDAR-induced fEPSPs' I–O curves, measured in slices from *Apoer2* KO mice or PP2-treated slices, were significantly decreased compared with the respective controls (Fig. 5 D and E), suggesting a decrease in the efficacy of NMDAR-mediated neurotransmission. Collectively, these data show that the disruption of the Reelin-Apoer2-SFKs pathway prevents ketamine's effects by removing a permissive condition likely due to the impairment of baseline NMDAR-mediated postsynaptic responses (*SI Appendix*, Fig. S5).

Discussion

In this study, we demonstrate that genetically deleted or pharmacologically inhibited Reelin, the Reelin receptor Apoer2, or downstream SFK signaling prevents the ketamine-induced, antidepressant-like behavioral changes and synaptic potentiation in the CA1
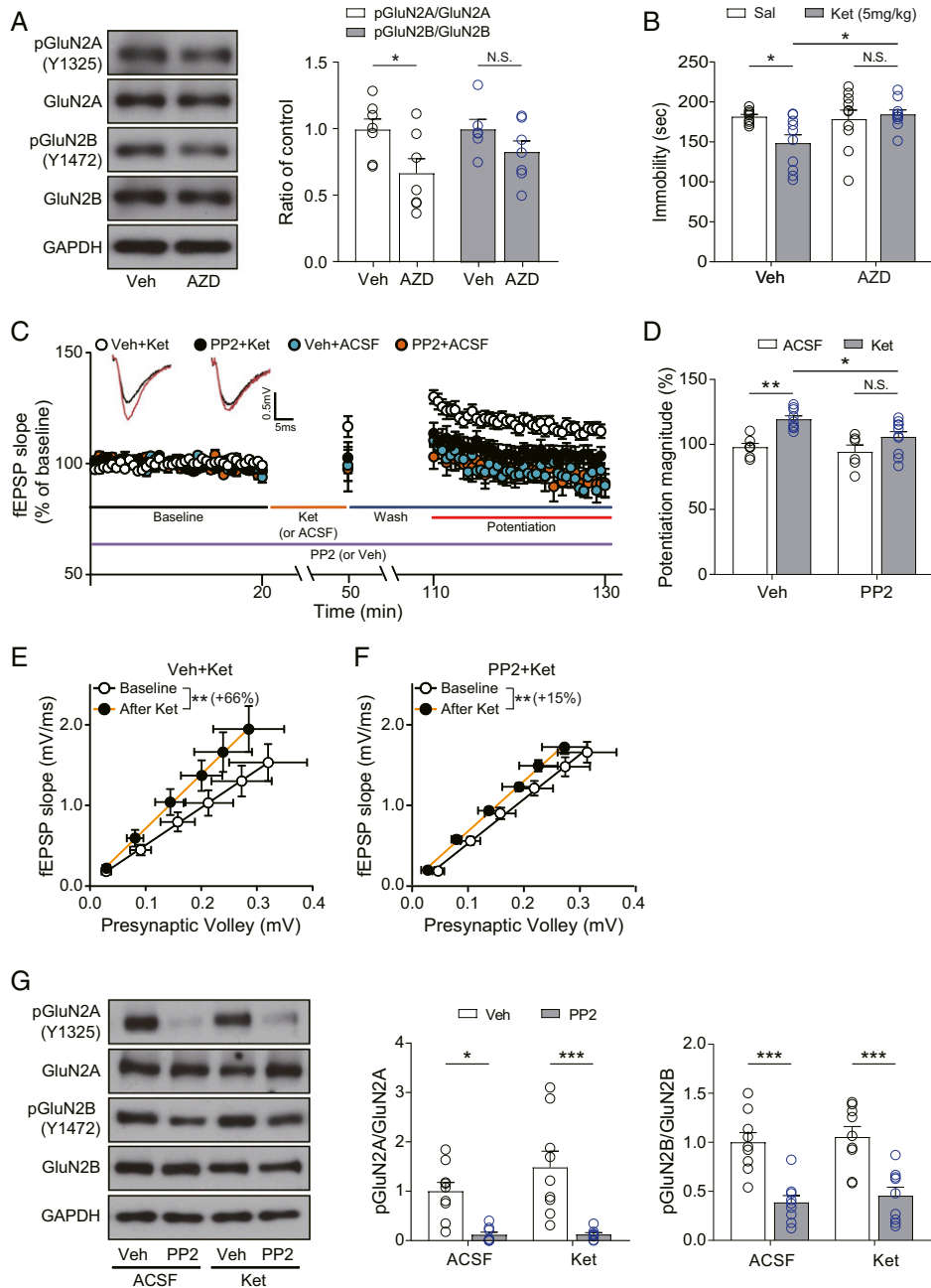
NEUROSCIENCE

Fig. 3. SFKs inhibition abolishes ketamine-mediated behavioral changes and synaptic potentiation. (*A*) Western blots and quantification showing GluN2A phosphorylation but not GluN2B phosphorylation was significantly decreased by AZD treatment [unpaired *t* test, pGluN2A/GluN2A: $t_{(12)}$ = 2.423, P = 0.0322; pGluN2B/GluN2B: $t_{(11)}$ = 1.459, P = 0.1727, *n* = 6 to 7 per group]. (*B*) Accumulated time the mice spent immobile during the FST performed 2 h after ketamine injection. AZD was injected 30 min before the ketamine injection. Pretreatment of AZD prevented the significant reduction of immobility by ketamine [two-way ANOVA with Tukey's multiple comparisons, AZD × ketamine: $F_{(1, 35)}$ = 5.285, P = 0.0276, AZD: $F_{(1, 35)}$ = 3.740, P = 0.0613, ketamine: $F_{(1, 35)}$ = 2.514, P = 0.1218, *n* = 9 to 10 per group]. (*C*) Ketamine potentiation was measured after 20 min of baseline measurement, 30 min of ketamine perfusion, and 1 h of washout period in the hippocampal CA1 region. PP2 was applied for the whole duration of the experiment. All responses were normalized to respective baselines. (*Inset*) Representative waveforms during baseline (black) or ketamine potentiation (red) measurement. (*D*) A bar graph that summarizes the magnitudes of ketamine potentiation of respective groups measured in *C*. PP2 prevented the significant increase of potentiation magnitude induced by ketamine [two-way ANOVA with Tukey's multiple comparisons, PP2 × ketamine: $F_{(1, 28)}$ = 1.706, P = 0.2021, PP2: $F_{(1, 28)}$ = 5.095, P = 0.0320, ketamine: $F_{(1, 28)}$ = 18.51, P = 0.0002, *n* = 6 to 10 per group]. (*E* and *F*) I–O curves measured during baseline and potentiation measurement in *C*. Initial slopes of fEPSPs versus presynaptic volley values are plotted at 4, 8, 12, 16, 20, and 24 μA stimulation intensity. The slope of the I–O curve was significantly increased after ketamine treatment in both the vehicle-treated slices and the PP2-treated slices [Wilcoxon matched-pairs signed rank test, DMSO+Ket (*E*): P = 0.0039, *n* = 9; PP2+Ket (*F*): P = 0.0117, *n* = 9]. However, the increase rate of the slope following ketamine perfusion was 66% in the Veh+Ket group but reduced to 15% in the PP2+Ket group. (*G*) Western blots and quantification of GluN2A, GluN2B, and their respective phosphorylation forms. Samples were collected after completion of recording in *C*. GluN2A and GluN2B phosphorylation were significantly decreased by PP2 treatment regardless of ketamine treatment, confirming the pharmacological effects of PP2 [two-way ANOVA with Tukey's multiple comparisons, pGluN2A/GluN2A—PP2 × ketamine: $F_{(1, 30)}$ = 1.373, P = 0.2505, PP2: $F_{(1, 30)}$ = 30.32, P < 0.0001, ketamine: $F_{(1, 30)}$ = 1.452, P = 0.2376, pGluN2B/GluN2B—PP2 × ketamine: $F_{(1, 32)}$ = 0.0051, P = 0.9431, PP2: $F_{(1, 32)}$ = 43.67, P < 0.0001, ketamine: $F_{(1, 32)}$ = 0.4409, P = 0.5114, *n* = 8 to 9 per group]. All data represented as mean ± SEM; *P < 0.05, **P < 0.01, and ***P < 0.001.
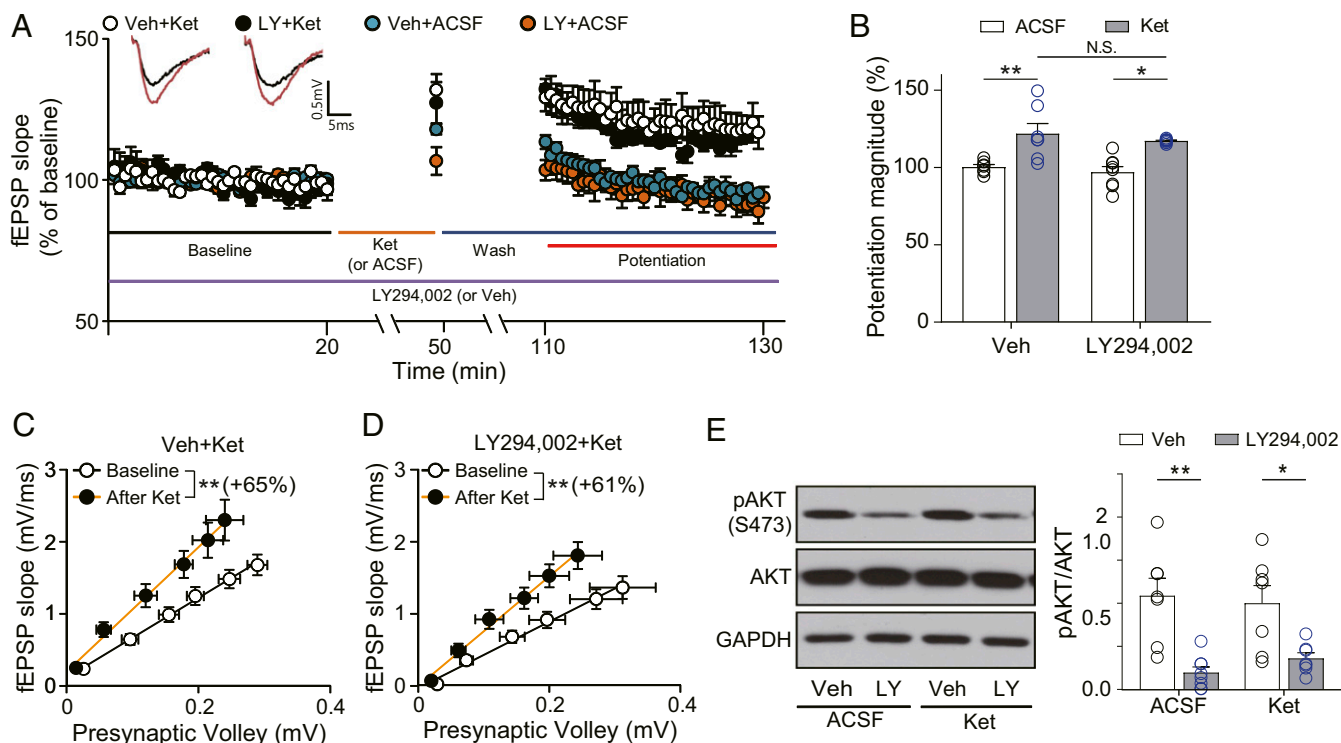
Fig. 4. PI3K inhibition does not affect ketamine potentiation. (*A*) Ketamine potentiation was measured after 20 min of baseline measurement, 30 min of ketamine perfusion, and 1 h of washout period in the hippocampal CA1 region. LY294002 was applied for the whole duration of the experiment. All responses were normalized to respective baselines. (*Inset*) Representative waveforms during baseline (black) or ketamine potentiation (red) measurement. (*B*) A bar graph that summarizes the magnitudes of ketamine potentiation of respective groups measured in *A*. LY294002 did not affect synaptic potentiation induced by ketamine [two-way ANOVA with Tukey's multiple comparisons, LY294002 × ketamine: $F_{(1, 25)} = 0.3351$, $P = 0.5678$, LY294002: $F_{(1, 25)} = 0.661$, $P = 0.4239$, ketamine: $F_{(1, 25)} = 27.23$, $P < 0.0001$, $n = 7$ to 8 per group]. (*C* and *D*) I–O curves measured during baseline and potentiation measurement in *A*. Initial slopes of fEPSPs versus presynaptic volley values are plotted at 4, 8, 12, 16, 20, and 24 μA stimulation intensity. The slope of the I–O curve was significantly increased after ketamine treatment in both the vehicle-treated and the LY294002-treated slices with similar increase rates [Paired *t* test, DMSO+Ket (*C*): $t_{(6)} = 3.737$, $P = 0.0097$, $n = 7$; LY294002+Ket (*D*): $t_{(6)} = 4.528$, $P = 0.0040$, $n = 7$]. (*E*) Western blots and quantification of AKT and pAKT. Samples were collected after completion of the recording in *A*. AKT phosphorylation was significantly decreased by LY294002 treatment regardless of ketamine treatment, confirming the pharmacological effects of LY294002 [two-way ANOVA with Tukey's multiple comparisons, LY294002 × ketamine: $F_{(1, 25)} = 0.7331$, $P = 0.4000$, LY294002: $F_{(1, 25)} = 26.89$, $P < 0.0001$, ketamine: $F_{(1, 25)} = 0.0690$, $P = 0.795$, $n = 7$ to 8 per group]. All data represented as mean ± SEM; *$P < 0.05$ and **$P < 0.01$.

hippocampal region. Notably, ketamine does not activate the Reelin-dependent signaling pathway. Instead, we found that NMDAR function is depressed when Apoer2 or SFKs are disrupted. Thus, these results suggest that Reelin-Apoer2-SFKs–mediated signaling is a key permissive factor of ketamine's antidepressant efficacy, possibly by maintaining proper baseline NMDAR function. These results provide important insights into understanding the synaptic mechanisms that may render patients nonresponsive to ketamine's antidepressant action.

Previous work has demonstrated that ketamine is a use-dependent NMDAR antagonist, in that the NMDAR must be first activated (or opened) for ketamine to block NMDARs (49). Therefore, depressed basal NMDAR activity would be expected to occlude ketamine's pharmacological action. Accordingly, we found that disruption of Apoer2 or SFKs depresses basal NMDAR function, suggesting that intact Apoer2-SFKs signaling is required to maintain normal NMDAR activity. In contrast, we found that impaired Reelin-Apoer2-SFKs pathway components did not affect the I–O curve slopes, compared with the respective control group, suggesting basal neurotransmission composed of AMPAR response is intact. Consistent with our results, previous studies have shown that each factor of the Reelin-Apoer2-SFKs pathway regulates NMDAR activity, respectively. Reelin activates NMDAR function by binding to its receptor, Apoer2, and activating SFKs (35, 37). Apoer2 regulates the phosphorylation and function of NMDARs by binding to NMDAR subunits, as well as activating its downstream

signaling SFKs (34, 35, 56). SFKs phosphorylate NMDAR subunits (GluN2A and GluN2B) and increase receptor function by enhancing the open probability of NMDAR channels (35, 37–39). Of note, application of Src, a subfamily of SFKs, in neurons directly activates NMDAR function and increases NMDAR Ca^{2+} currents by up-regulating overall tyrosine phosphorylation in GluN2A and GluN2B (38, 39, 57). Conversely, inhibition of SFKs has been shown to decrease NMDAR currents (50), consistent with our findings. These lines of evidence support the role of Reelin-Apoer2-SFKs pathway in maintaining basal NMDAR function. Therefore, one parsimonious conclusion is that the attenuated behavioral and synaptic effects by ketamine in the presence of impaired Reelin-Apoer2-SFKs pathway may be due to suppressed NMDAR function. However, we cannot rule out the possibility that other instructive factors that are regulated by the Reelin-Apoer2-SFKs pathway may be involved in ketamine-mediated effects.

Earlier studies raised the question of whether ketamine's rapid antidepressant effects are induced by NMDAR antagonism. It was suggested that a ketamine metabolite, (2R, 6R)-hydroxynorketamine, was NMDAR-independent and essential for ketamine's rapid antidepressant effects (58). However, in the same study, it was shown that deuterated ketamine at the C6 position, which is a metabolically stabilized form, produces rapid antidepressant effects, suggesting that ketamine is critical for the antidepressant effects (58). Our previous work demonstrated that (2R, 6R)-hydroxynorketamine blocks
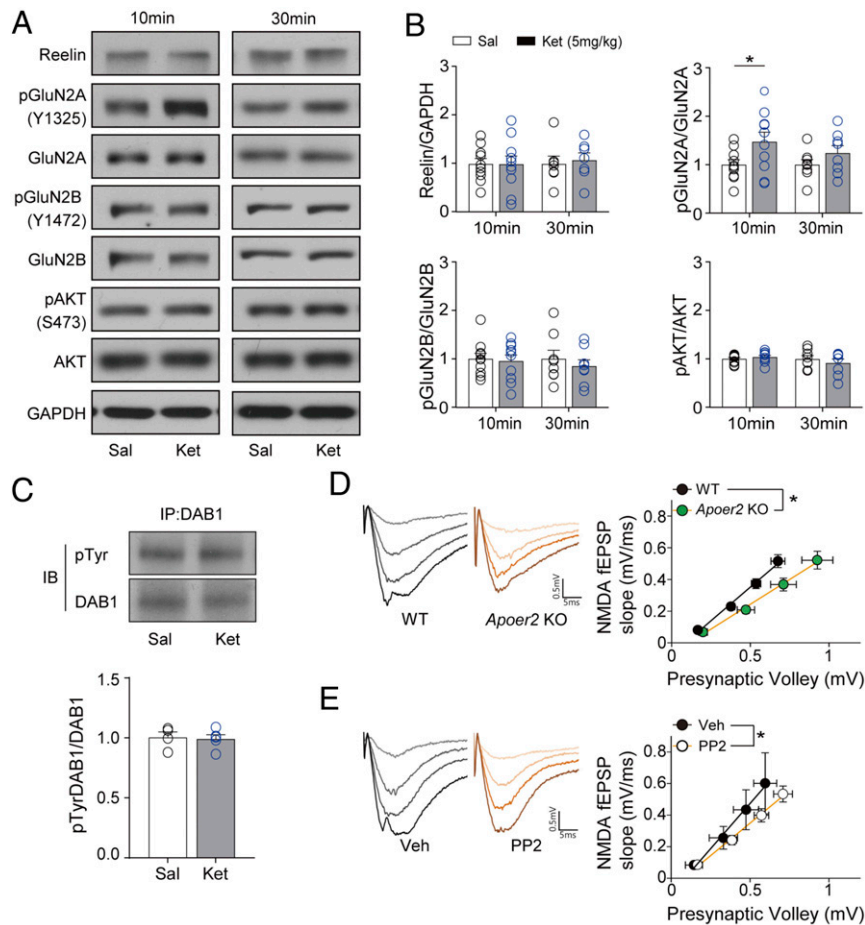
NEUROSCIENCE

Fig. 5. Disruption of Apoer2 and SFKs depresses NMDAR function. (*A* and *B*) Western blots and quantification showing changes of protein and phosphorylation in the hippocampus 10 min or 30 min after ketamine injection. (*B*) GluN2A phosphorylation was significantly increased 10 min after ketamine injection but returned to the control level 30 min after injection. But any significant changes were not observed in the level of Reelin, pGluN2B, and pAKT at 10 and 30 min after ketamine i.p. injection [unpaired *t* test, pGluN2A/GluN2A—10 min: $t_{(18)} = 2.133$, $P = 0.0470$, 30 min: $t_{(14)} = 1.292$, $P = 0.2173$; Reelin—10 min: $t_{(18)} = 0.0266$, $P = 0.9791$, 30 min: $t_{(12)} = 0.3503$, $P = 0.7322$; pGluN2B/GluN2B—10 min: $t_{(18)} = 0.2721$, $P = 0.7887$, 30 min: $t_{(14)} = 0.6826$, $P = 0.5060$; pAKT/AKT—10 min: $t_{(18)} = 0.8431$, $P = 0.4103$, 30 min: $t_{(14)} = 0.7883$, $P = 0.4436$, $n = 7$ to 10 per group]. (*C*) Tyrosine phosphorylation was examined after immunoprecipitation with DAB1 antibody in the hippocampal lysate. Samples were collected 10 min after ketamine treatment. Ketamine did not change the tyrosine phosphorylation of DAB1 [unpaired *t* test, $t_{(7)} = 0.2300$, $P = 0.8246$, $n = 4$ and 5 for saline and ketamine group, respectively]. (*D*) The slope of the NMDA I–O curve was significantly decreased in slices from *Apoer2* KO mice compared with slices from WT mice [unpaired *t* test, $t_{(22)} = 2.652$, $P = 0.0146$, $n = 11$ and 13 for WT and *Apoer2* KO, respectively]. (*E*) The slope of the NMDA I–O curve was significantly decreased in PP2-treated slices, compared with vehicle-treated slices [unpaired *t* test, $t_{(22)} = 2.430$, $P = 0.0237$, $n = 10$ and 14 for Veh and PP2, respectively]. All data represented as mean ± SEM; *$P < 0.05$.

NMDAR activity (59), suggesting that the NMDAR blockade is still involved in the antidepressant effects induced by (2R, 6R)-hydroxynorketamine (but also see ref. 60). Previous work has also shown that the antidepressant effects and molecular changes induced by ketamine were occluded in a genetic mouse model lacking GluN2A globally or in paralbumin interneurons or lacking GluN2B in excitatory neurons of broad forebrain regions, including the hippocampus (61, 62). While there have been other hypotheses regarding the NMDAR-independent antidepressant effects of ketamine (58, 63), there is no mechanistic intracellular signaling pathway that has been suggested to underlie the effects. Ketamine likely has many effects in the central nervous system, but not all of them are linked to rapid antidepressant action. Another compelling reason for the role of NMDARs in ketamine's antidepressant efficacy is the comparison of the pharmacodynamic property and antidepressant efficacy between enantiomers of ketamine. Ketamine is a racemic mixture of (R)- and (S)-ketamine. (S)-ketamine has a four times higher binding affinity to the NMDAR than (R)-ketamine. Recently, (S)-ketamine has been clinically proven for its antidepressant efficacy (64) and now is approved by the Food

and Drug Administration for treatment-resistant depression (65). Taken together, these lines of evidence and our current findings show that NMDAR antagonism is essential to exert ketamine's rapid antidepressant effects.

In our results, inhibition of PI3K does not affect ketamine-induced synaptic potentiation, indicating that disruption of spontaneous neurotransmitter release driven by PI3K-AKT-VAMP7 (31) is not involved in the mechanism underlying ketamine's antidepressant effects. However, given that the ablation of both VAMP7 and Vti1a prevents the ketamine-induced synaptic potentiation (32), we cannot rule out that the disruption of the PI3K-AKT-VAMP7 pathway alone is insufficient to affect ketamine's effects. Indeed, it is possible there may be additional presynaptic molecules that regulate ketamine-induced synaptic plasticity. This possibility awaits further investigation.

In the current study, we observed a transient increase in GluN2A phosphorylation by ketamine. This result raises the possibility that ketamine may rapidly activate Reelin-dependent SFKs. However, the increased levels of phospho-GluN2A are not likely mediated either by increased Reelin expression or secretion. Specifically, we

did not see a change in the level of Reelin expression after ketamine treatment, suggesting that ketamine does not change the translation of Reelin within this relatively rapid time frame. In addition, Reelin has been suggested to be secreted through a constitutive pathway and not a regulated pathway. The secretion of Reelin has been shown to be affected by its synthesis and not neural activity or transmitter release (66). Lastly, we did not see any changes in the phosphorylation of DAB1, a key adaptor molecule to mediate activation of Reelin-dependent signaling (35, 67, 68). Thus, presumably, other factors may be involved in the transiently increased phosphorylation of GluN2A (69, 70). Of note, we cannot rule out a possibility that ketamine-induced activation of SFKs, which thereby increases NMDAR phosphorylation, could contribute to ketamine's effects through parallel mechanisms in addition to Reelin signaling.

Previous work has reported that ketamine treatment rescues impairments in juvenile heterozygous reeler mice, including spine morphology, synaptic transmission abnormalities in the prelimbic prefrontal cortex (e.g., long-term potentiation, AMPAR spontaneous excitatory postsynaptic currents [sEPSCs], and NMDAR sEPSCs), and memory renewal behaviors (71, 72). Although these studies seem to contradict our findings of the abolished ketamine's effects in *Reelin* cKO mice, there are several key experimental differences between the current study and previous work. In the current study, we used low-dose ketamine (5 mg/kg), compared with the previous studies in which ketamine rescued the impairments observed in juvenile heterozygote reeler mice robustly at 100 mg/kg but only weakly at 30 mg/kg. The 100 mg/kg ketamine is close to the anesthetic dose in mice, while 3 to 10 mg/kg ketamine is typically used to examine antidepressant effects in mice (16, 22, 27, 58). Previous work has shown that ketamine does not produce antidepressant effects at higher doses (over 20 mg/kg) (22, 58), and these higher doses do not activate the molecular signaling and synaptic changes observed with the low doses (22). Therefore, the observations in the previous work may not necessarily be due to the antidepressant effects of ketamine. Another key difference is that we used adult mice in the current study, while the previous study showed the therapeutic effects of ketamine in juvenile heterozygous reeler mice (P22 to P28) (71, 72), although ketamine-mediated, rapid antidepressant-like behavioral changes and synaptic potentiation are not observed in juvenile mice (20). The earlier work also examined changes in the prefrontal cortex, while our findings examined in the hippocampus. These key differences in experimental conditions may explain the differences in ketamine effects in heterozygous reeler mice in the previous studies (71, 72) and in *Reelin* cKO mice in our current findings.

In the current study, we assessed synaptic, biochemical, and behavioral techniques to examine the role of Reelin signaling in ketamine's antidepressant action. The behavioral effects of ketamine were assessed using the FST, a reproducible and robust paradigm that recapitulates ketamine's fast-acting antidepressant action (16). Previous studies support the predictive and face validities of the FST for ketamine-mediated, antidepressive behavioral changes (16, 25–27, 42), although this paradigm lacks face and constructive validities as an animal model of depression (73). In future studies, it will be important to investigate the effects of ketamine on stress-induced behavioral changes such as anhedonia, social avoidance, and anxiety in mice with deficient Reelin-Apoer2-SFKs signaling. This analysis may elucidate whether ketamine is rescuing depressive-like behavior or activates homeostatic pathways to compensate for the underlying pathology (24).

The results of this study provide critical information on potential factors that may underlie the lack of antidepressant responsiveness to ketamine administration. As demonstrated here, disruption of Reelin and its downstream signaling interferes with ketamine's antidepressant action. Interestingly, disrupted Reelin expression has been observed in some patients with MDD (74). While the source of Reelin in the mature nervous system remains poorly understood, there is evidence for Reelin expression in somatostatin-expressing GABAergic neurons in the forebrain (75, 76). Taken together, our results show that components of the Reelin-Apoer2-SFKs pathway act as key permissive factors required for ketamine's antidepressant effects and baseline regulation of NMDAR activity, thus functioning as determinants of ketamine's antidepressant efficacy.

Materials and Methods

Mice. *Reelin* cKO mice were generated as described previously (40). Briefly, the first exon of the *Reelin* gene was flanked by loxP, and heterozygous *Reelin$^{flox/wt}$* mice were crossed with CAG-CreERT2 mice, which have a mutated estrogen receptor activated by tamoxifen treatment (77). To induce the Cre-lox recombination, tamoxifen was given for 5 d at 2 mo of age after the developmental period. Approximately 1 to 2 mo after tamoxifen injection, the mice were used for this study.

Apoer2 KO mice were generated as described previously (44). For *Apoer2* KO mutation, exons 17 and 18 were substituted with a pol neo cassette. To get *Apoer2* WT and KO mice, *Apoer2* heterozygous male and female mice were mated.

For control mice, C57BL/6J male mice were used for this study. In all experiments, animals aged 2 to 6 mo old were used, and age-matched littermate control and KO animals were used for respective experiments. Animals were maintained on a 12 h-light/12 h-dark cycle at ambient temperature (23 ± 3 °C) and humidity (50 ± 20%), with free access to chow pellets and water. All animal procedures were performed following the *Guide for the Care and Use of Laboratory Animals* (78) and were approved by the institutional animal care and use committee at University of Texas Southwestern Medical Center or Vanderbilt University.

Drugs. The dosage of drugs was used as follows: for behavior studies, ketamine 5 mg/kg (Hospira) and AZD 20 mg/kg (Apexbio) and for field recording experiments, ketamine 20 μM (Hospira), PP2 10 μM (Apexbio), AZD 5 μM (Apexbio), and LY294002 10 μM (Apexbio).

Forced Swim Test. Before the FST, mice had been habituated to experimenter's handling for 2 wk (1 min per mouse). A mouse was placed in a 4 L Pyrex glass beaker containing 3 L water (23 to 25 °C) for 6 min after 2 h of saline or ketamine treatment. For the SFKs inhibitor experiment, AZD or its vehicle (5% DMSO in saline) was administrated 30 min before the ketamine treatment. The accumulated immobility time was measured during the last 4 min except for the first 2 min. The water was changed in each trial.

NSFT. Group-housed animals fasted overnight before the test. On the day of the test, animals were transferred to a testing room and habituated for 2 h. For each trial, a fresh food pellet was placed in the middle of a 42 × 42 cm open-field arena. Approximately 2 h after ketamine treatment, a mouse was placed in a corner of the arena and allowed to explore for up to 8 min. The trial was immediately ended when the mouse chewed a part of chow, and the latency to feed was recorded. Then, the mouse was transferred to the clean cage with a new food pellet and allowed to eat for 5 min. The consumed weight of the pellet was recorded to investigate the change of appetite.

Brain Tissue Preparation. Whole brains were sliced (~1 mm thick per slice) using an ice-chilled matrix for the coronal dissection of the mouse brain (Alto acrylic 1 mm mouse brain coronal, AL-1175). In this setting, two to three hippocampal slices in the rostral direction were collected. These hippocampal slices were extracted from both the dorsal and ventral hippocampus. The slices were immediately frozen and lysed using a radioimmunoprecipitation assay buffer (50 mM Tris, pH 7.4, 1% Igepal, 0.1% SDS, 0.5% Na deoxycholate, 4 mM EDTA, 150 mM NaCl, cOmplete™, mini protease inhibitor cocktail [11836153001, Roche], and phosSTOP™ [4906845001, Roche]). The total protein amount was quantified by bicinchoninic acid (BCA) analysis and diluted with 2× Laemmli sample buffer (Bio-Rad). The prepared samples were boiled at 95 °C for 7 min and stored at −20 °C for further experiments.

Immunoprecipitation. Tissues were lysed with lysis buffer (50 mM Tris pH7.4, 150 mM NaCl, 5 mM EDTA, 1% Nonidet P-40, 0.5% deoxycholic acid, 0.1% SDS, cOmplete™,mini protease inhibitorcocktail, and phosSTOP™ [Roche]). The protein amount was quantified with BCA analysis. The same amount of protein was transferred into new tubes. The transferred lysate was incubated with 20 μL protein G in 1% BSA at 4 °C for 1 h. After the samples were centrifuged for 14,000 × g for 10 min, the supernatant was transferred and subjected to immunoprecipitation with anti-mouse DAB1 at 4 °C overnight.

Kim et al.
A key requirement for synaptic Reelin signaling in ketamine-mediated behavioral and synaptic action

PNAS | 9 of 11
https://doi.org/10.1073/pnas.2103079118

The next day, the samples were incubated with 20 μL protein G at 4 °C for 3 h. The samples were washed three times with lysis buffer and resuspended in 2× SDS sample buffer. The prepared samples were boiled at 95 °C for 7 min, centrifuged, and stored at −20 °C for further experiments.

Western Blot. The same amount of total protein per well was loaded on SDS-polyacrylamide gel electrophoresis gels and then transferred to nitrocellulose membranes. The membranes were incubated for 1 h at room temperature in blocking solution (0.1% TBST: 5% skim milk in Tris-buffered saline with 0.1% Tween). Blots were incubated overnight at 4 °C with the following primary antibodies: anti-phosphotyrosine (4G10, 05-321, MilliporeSigma), anti–phospho-NMDAR2B (Y1472, 4208, cell signaling technology), anti–phospho-NMDAR2A (Y1325, ab16646, Abcam), anti-NMDAR2A (06-313, upstate), anti-NMDAR2B (06-600, upstate), anti-GAPDH (2118, cell signaling technology), anti–phosphor-AKT (S473, 9271, cell signaling technology), and anti-AKT (9272, cell signaling technology); anti-Reelin and anti-DAB1 were kind gifts from Dr. Joachim Herz. After three times of washing with 0.1% TBST, blots were incubated with secondary antibodies at room temperature for 2 h. Protein bands were detected with enhanced chemiluminescence (Bio-Rad) and visualized by exposing the blots to X-ray film.

Hippocampal Field Recording. The brain was removed, dissected, and then sliced using a vibratome (VT1000 S, Leica) in ice-cold dissection buffer (2.6 mM KCl, 1.25 mM NaH_2PO_4, 26 mM $NaHCO_3$, 0.5 mM $CaCl_2$, 5 mM $MgCl_2$, 212 mM sucrose, and 10 mM glucose). ACSF and dissection buffer were equilibrated with 95% O_2 and 5% CO_2. Area CA3 was surgically removed from each slice immediately after sectioning. The slices were transferred into a reservoir chamber filled with ACSF containing the following: 124 mM NaCl, 5 mM KCl, 1.25 mM NaH_2PO_4, 26 mM $NaHCO_3$, 2 mM CaCl2, 2 mM $MgCl_2$, and 10 mM glucose. Slices were allowed to recover for 2 to 3 h at 30 °C. For recording, slices were transferred to a submerged recording chamber, maintained at 30 °C, and perfused continuously with ACSF at a rate of 2 to 3 mL/min. fEPSPs were evoked by stimulation of Schaffer collateral/commissural afferents with a concentric bipolar microelectrode (CBBRC75, FHC) and recorded with extracellular recording electrodes filled with ACSF and placed in stratum radiatum of area CA1. A stable baseline was collected every 30 s using a stimulus yielding 50 to 75% of the maximum peak. A stable baseline was determined by confirming the lack of sustained fluctuations over several trials in the value of fEPSP slopes for 20 min of recording. Then, I–O response was measured to figure out the response intensity using 4, 8, 12, 16, 20, and 24 μA stimulation before and after ketamine treatment. To describe the presynaptic functional changes, PPRs were

measured with interstimulus intervals of 20, 30, 50, 100, 200, 400, and 500 ms before and after ketamine treatment. NMDAR-driven fEPSPs were recorded in solution containing 124 mM NaCl, 2 mM KCl, 3 mM $CaCl_2$, 0.1 mM $MgCl_2$, 10 mM Glucose, 1.2 mM NaH_2PO_4, 26 mM $NaHCO_3$, and 0.02 mM 6,7-dinitroquinoxaline-2,3-dione. After 20 min of stable baseline, the initial slope of fEPSP versus presynaptic volley value was measured at 10, 20, 30, and 40 μA stimulation intensity to analyze the I–O curve relationship.

Ketamine potentiation was measured as previously described (19). After measuring the baseline response for 20 min, ketamine (20 μM) or ACSF was perfused with a rate of 3 mL/min without recording for 30 min. After the ketamine perfusion, single stimulation was applied to examine the potentiated response. After 1 h washout period, the recording was resumed for a further 20 min to confirm the continuation of the potentiation. For inhibitor experiments, ACSF containing PP2 (10 μM), LY294002 (10 μM), or AZD (5 μM) was perfused continuously during the whole recording period.

Statistical Analysis. All data were analyzed with GraphPad Prism 8.4.3 software. The normal distribution of data was analyzed with the Shapiro–Wilk test ($n < 8$) or D'Agostino and Pearson test ($n \geq 8$). When data follow a normal distribution, parametric statistical analysis was used. If not, data were transformed with the Box–Cox transformation with SPC for Excel software, or nonparametric statistical analyses were used. For the comparison between two groups, unpaired or paired t test, Mann–Whitney test, or Wilcoxon matched-pairs signed rank test was used. In datasets with two independent variables, two-way ANOVA followed by Tukey's multiple comparisons post hoc test was used. Comparisons were considered to be statistically significant when $P < 0.05$.

Data Availability. All study data are included in the article and/or *SI Appendix*.

1. D. S. Hasin *et al.*, Epidemiology of adult DSM-5 major depressive disorder and its specifiers in the United States. *JAMA Psychiatry* **75**, 336–346 (2018).
2. M. Fava, K. G. Davidson, Definition and epidemiology of treatment-resistant depression. *Psychiatr. Clin. North Am.* **19**, 179–200 (1996).
3. B. N. Gaynes *et al.*, What did STAR*D teach us? Results from a large-scale, practical, clinical trial for patients with depression. *Psychiatr. Serv.* **60**, 1439–1445 (2009).
4. R. M. Berman *et al.*, Antidepressant effects of ketamine in depressed patients. *Biol. Psychiatry* **47**, 351–354 (2000).
5. C. A. Zarate Jr. *et al.*, A randomized trial of an N-methyl-D-aspartate antagonist in treatment-resistant major depression. *Arch. Gen. Psychiatry* **63**, 856–864 (2006).
6. J. W. Murrough *et al.*, Antidepressant efficacy of ketamine in treatment-resistant major depression: A two-site randomized controlled trial. *Am. J. Psychiatry* **170**, 1134–1142 (2013).
7. N. D. Iadarola *et al.*, Ketamine and other N-methyl-D-aspartate receptor antagonists in the treatment of depression: A perspective review. *Ther. Adv. Chronic Dis.* **6**, 97–114 (2015). Correction in: *Ther. Adv. Chronic Dis.* **7**, 184 (2016).
8. G. M. MacQueen *et al.*, Course of illness, hippocampal function, and hippocampal volume in major depression. *Proc. Natl. Acad. Sci. U.S.A.* **100**, 1387–1392 (2003).
9. M. Vythilingam *et al.*, Childhood trauma associated with smaller hippocampal volume in women with major depression. *Am. J. Psychiatry* **159**, 2072–2080 (2002).
10. Y. I. Sheline, P. W. Wang, M. H. Gado, J. G. Csernansky, M. W. Vannier, Hippocampal atrophy in recurrent major depression. *Proc. Natl. Acad. Sci. U.S.A.* **93**, 3908–3913 (1996).
11. J. L. Beyer, K. R. R. Krishnan, Volumetric brain imaging findings in mood disorders. *Bipolar Disord.* **4**, 89–104 (2002).
12. S. Campbell, G. Macqueen, The role of the hippocampus in the pathophysiology of major depression. *J. Psychiatry Neurosci.* **29**, 417–426 (2004).
13. G. MacQueen, T. Frodl, The hippocampus in major depression: Evidence for the convergence of the bench and bedside in psychiatric research? *Mol. Psychiatry* **16**, 252–264 (2011).
14. Y. I. Sheline, M. H. Gado, H. C. Kraemer, Untreated depression and hippocampal volume loss. *Am. J. Psychiatry* **160**, 1516–1518 (2003).
15. I. Herrera-Guzmán *et al.*, Effects of selective serotonin reuptake and dual serotonergic-noradrenergic reuptake treatments on memory and mental processing speed in patients with major depressive disorder. *J. Psychiatr. Res.* **43**, 855–863 (2009).

16. A. E. Autry *et al.*, NMDA receptor blockade at rest triggers rapid behavioural antidepressant responses. *Nature* **475**, 91–95 (2011).
17. J.-W. Wang, D. J. David, J. E. Monckton, F. Battaglia, R. Hen, Chronic fluoxetine stimulates maturation and synaptic plasticity of adult-born hippocampal granule cells. *J. Neurosci.* **28**, 1374–1384 (2008).
18. F. R. Carreno *et al.*, Activation of a ventral hippocampus-medial prefrontal cortex pathway is both necessary and sufficient for an antidepressant response to ketamine. *Mol. Psychiatry* **21**, 1298–1308 (2016).
19. E. Nosyreva *et al.*, Acute suppression of spontaneous neurotransmission drives synaptic potentiation. *J. Neurosci.* **33**, 6990–7002 (2013).
20. E. Nosyreva, A. E. Autry, E. T. Kavalali, L. M. Monteggia, Age dependence of the rapid antidepressant and synaptic effects of acute NMDA receptor blockade. *Front. Mol. Neurosci.* **7**, 94 (2014).
21. E. S. Gideons, E. T. Kavalali, L. M. Monteggia, Mechanisms underlying differential effectiveness of memantine and ketamine in rapid antidepressant responses. *Proc. Natl. Acad. Sci. U.S.A.* **111**, 8649–8654 (2014).
22. J.-W. Kim, L. M. Monteggia, Increasing doses of ketamine curtail antidepressant responses and suppress associated synaptic signaling pathways. *Behav. Brain Res.* **380**, 112378 (2020).
23. E. T. Kavalali, L. M. Monteggia, Synaptic mechanisms underlying rapid antidepressant action of ketamine. *Am. J. Psychiatry* **169**, 1150–1156 (2012).
24. E. T. Kavalali, L. M. Monteggia, Targeting homeostatic synaptic plasticity for treatment of mood disorders. *Neuron* **106**, 715–726 (2020).
25. R.-J. Liu *et al.*, Brain-derived neurotrophic factor Val66Met allele impairs basal and ketamine-stimulated synaptogenesis in prefrontal cortex. *Biol. Psychiatry* **71**, 996–1005 (2012).
26. G. Laje *et al.*, Brain-derived neurotrophic factor Val66Met polymorphism and antidepressant efficacy of ketamine in depressed patients. *Biol. Psychiatry* **72**, e27–e28 (2012).
27. S. Maeng *et al.*, Cellular mechanisms underlying the antidepressant effects of ketamine: Role of alpha-amino-3-hydroxy-5-methylisoxazole-4-propionic acid receptors. *Biol. Psychiatry* **63**, 349–352 (2008).
28. A. L. Reese, E. T. Kavalali, Spontaneous neurotransmission signals through store-driven Ca(2+) transients to maintain synaptic homeostasis. *eLife* **4**, e09262 (2015).

29. D. Atasoy et al., Spontaneous and evoked glutamate release activates two populations of NMDA receptors with limited overlap. J. Neurosci. 28, 10151–10166 (2008).

30. D. M. O. Ramirez, M. Khvotchev, B. Trauterman, E. T. Kavalali, Vti1a identifies a vesicle pool that preferentially recycles at rest and maintains spontaneous neurotransmission. Neuron 73, 121–134 (2012).

31. M. Bal et al., Reelin mobilizes a VAMP7-dependent synaptic vesicle pool and selectively augments spontaneous neurotransmission. Neuron 80, 934–946 (2013).

32. D. C. Crawford, D. M. O. Ramirez, B. Trauterman, L. M. Monteggia, E. T. Kavalali, Selective molecular impairment of spontaneous neurotransmission modulates synaptic efficacy. Nat. Commun. 8, 14436 (2017).

33. T. Hiesberger et al., Direct binding of Reelin to VLDL receptor and ApoE receptor 2 induces tyrosine phosphorylation of disabled-1 and modulates tau phosphorylation. Neuron 24, 481–489 (1999).

34. U. Beffert et al., Modulation of synaptic plasticity and memory by Reelin involves differential splicing of the lipoprotein receptor Apoer2. Neuron 47, 567–579 (2005).

35. H. H. Bock, J. Herz, Reelin activates SRC family tyrosine kinases in neurons. Curr. Biol. 13, 18–26 (2003).

36. E. J. Weeber et al., Reelin and ApoE receptors cooperate to enhance hippocampal synaptic plasticity and learning. J. Biol. Chem. 277, 39944–39952 (2002).

37. Y. Chen et al., Reelin modulates NMDA receptor activity in cortical neurons. J. Neurosci. 25, 8209–8216 (2005).

38. X. M. Yu, R. Askalan, G. J. Keil II, M. W. Salter, NMDA channel regulation by channel-associated protein tyrosine kinase Src. Science 275, 674–678 (1997).

39. Y. T. Wang, M. W. Salter, Regulation of NMDA receptors by tyrosine kinases and phosphatases. Nature 369, 233–235 (1994).

40. C. Lane-Donovan et al., Reelin protects against amyloid β toxicity in vivo. Sci. Signal. 8, ra67 (2015).

41. F. Tissir, A. M. Goffinet, Reelin and brain development. Nat. Rev. Neurosci. 4, 496–505 (2003).

42. C. A. Zarate Jr. et al., A double-blind, placebo-controlled study of memantine in the treatment of major depression. Am. J. Psychiatry 163, 153–155 (2006).

43. U. Beffert et al., Reelin-mediated signaling locally regulates protein kinase B/Akt and glycogen synthase kinase 3beta. J. Biol. Chem. 277, 49958–49964 (2002).

44. M. Trommsdorff et al., Reeler/Disabled-like disruption of neuronal migration in knockout mice lacking the VLDL receptor and ApoE receptor 2. Cell 97, 689–701 (1999).

45. O. M. Andersen, D. Benhayon, T. Curran, T. E. Willnow, Differential binding of ligands to the apolipoprotein E receptor 2. Biochemistry 42, 9355–9364 (2003).

46. N. Yasui, T. Nogi, J. Takagi, Structural basis for specific recognition of Reelin by its receptors. Structure 18, 320–331 (2010).

47. K. A. Stedenfeld et al., Novelty-seeking behavior predicts vulnerability in a rodent model of depression. Physiol. Behav. 103, 210–216 (2011).

48. M. S. Durakoglugil, Y. Chen, C. L. White, E. T. Kavalali, J. Herz, Reelin signaling antagonizes beta-amyloid at the synapse. Proc. Natl. Acad. Sci. U.S.A. 106, 15938–15943 (2009).

49. J. F. MacDonald, Z. Miljkovic, P. Pennefather, Use-dependent block of excitatory amino acid currents in cultured neurons by ketamine. J. Neurophysiol. 58, 251–266 (1987).

50. J. Xu et al., Control of excitatory synaptic transmission by C-terminal Src kinase. J. Biol. Chem. 283, 17503–17514 (2008).

51. E. J. Hennequin et al., N-(5-chloro-1,3-benzodioxol-4-yl)-7-[2-(4-methylpiperazin-1-yl)ethoxy]-5-(tetrahydro-2H-pyran-4-yloxy)quinazolin-4-amine, a novel, highly selective, orally available, dual-specific c-Src/Abl kinase inhibitor. J. Med. Chem. 49, 6465–6488 (2006).

52. A. C. Kaufman et al., Fyn inhibition rescues established memory and synapse loss in Alzheimer mice. Ann. Neurol. 77, 953–971 (2015).

53. M. Yang, J. P. Leonard, Identification of mouse NMDA receptor subunit NR2A C-terminal tyrosine sites phosphorylated by coexpression with v-Src. J. Neurochem. 77, 580–588 (2001).

54. T. Nakazawa et al., Characterization of Fyn-mediated tyrosine phosphorylation sites on GluR epsilon 2 (NR2B) subunit of the N-methyl-D-aspartate receptor. J. Biol. Chem. 276, 693–699 (2001).

55. M. W. Salter, L. V. Kalia, Src kinases: A hub for NMDA receptor regulation. Nat. Rev. Neurosci. 5, 317–328 (2004).

56. H.-S. Hoe et al., Apolipoprotein E receptor 2 interactions with the N-methyl-D-aspartate receptor. J. Biol. Chem. 281, 3425–3431 (2006).

57. Y. T. Wang, X. M. Yu, M. W. Salter, Ca(2+)-independent reduction of N-methyl-D-aspartate channel activity by protein tyrosine phosphatase. Proc. Natl. Acad. Sci. U.S.A. 93, 1721–1725 (1996).

58. P. Zanos et al., NMDAR inhibition-independent antidepressant actions of ketamine metabolites. Nature 533, 481–486 (2016).

59. K. Suzuki, E. Nosyreva, K. W. Hunt, E. T. Kavalali, L. M. Monteggia, Effects of a ketamine metabolite on synaptic NMDAR function. Nature 546, E1–E3 (2017).

60. E. W. Lumsden et al., Antidepressant-relevant concentrations of the ketamine metabolite (2R,6R)-hydroxynorketamine do not block NMDA receptor function. Proc. Natl. Acad. Sci. U.S.A. 116, 5160–5169 (2019).

61. O. H. Miller et al., GluN2B-containing NMDA receptors regulate depression-like behavior and are critical for the rapid antidepressant actions of ketamine. eLife 3, e03581 (2014).

62. N. Picard, A. E. Takesian, M. Fagiolini, T. K. Hensch, NMDA 2A receptors in parvalbumin cells mediate sex-specific rapid ketamine response on cortical activity. Mol. Psychiatry 24, 828–838 (2019).

63. N. R. Williams et al., Attenuation of antidepressant effects of ketamine by opioid receptor antagonism. Am. J. Psychiatry 175, 1205–1215 (2018).

64. E. J. Daly et al., Efficacy and safety of intranasal esketamine adjunctive to oral antidepressant therapy in treatment-resistant depression: A randomized clinical trial. JAMA Psychiatry 75, 139–148 (2018).

65. J. Kim, T. Farchione, A. Potter, Q. Chen, R. Temple, Esketamine for treatment-resistant depression–First FDA-approved antidepressant in a new class. N. Engl. J. Med. 381, 1–4 (2019).

66. P. N. Lacor et al., Reelin secretion from glutamatergic neurons in culture is independent from neurotransmitter regulation. Proc. Natl. Acad. Sci. U.S.A. 97, 3556–3561 (2000).

67. H. H. Bock et al., Phosphatidylinositol 3-kinase interacts with the adaptor protein Dab1 in response to Reelin signaling and is required for normal cortical lamination. J. Biol. Chem. 278, 38772–38779 (2003).

68. B. W. Howell, T. M. Herrick, J. A. Cooper, Reelin-induced tyrosine [corrected] phosphorylation of disabled 1 during neuronal positioning. Genes Dev. 13, 643–648 (1999).

69. Y. Iwasaki, B. Gay, K. Wada, S. Koizumi, Association of the Src family tyrosine kinase Fyn with TrkB. J. Neurochem. 71, 106–111 (1998).

70. M. A. Takasu, M. B. Dalva, R. E. Zigmond, M. E. Greenberg, Modulation of NMDA receptor-dependent calcium influx and gene expression through EphB receptors. Science 295, 491–495 (2002).

71. J. Iafrati et al., Multivariate synaptic and behavioral profiling reveals new developmental endophenotypes in the prefrontal cortex. Sci. Rep. 6, 35504 (2016).

72. J. Iafrati et al., Reelin, an extracellular matrix protein linked to early onset psychiatric diseases, drives postnatal development of the prefrontal cortex via GluN2B-NMDARs and the mTOR pathway. Mol. Psychiatry 19, 417–426 (2014).Correction in: Mol. Psychiatry 19, 527 (2014).

73. M. L. Molendijk, E. R. de Kloet, Immobility in the forced swim test is adaptive and does not reflect depression. Psychoneuroendocrinology 62, 389–391 (2015).

74. S. H. Fatemi, J. A. Earle, T. McMenomy, Reduction in Reelin immunoreactivity in hippocampus of subjects with schizophrenia, bipolar disorder and major depression. Mol. Psychiatry 5, 654–663, 571 (2000).

75. S. Alcántara et al., Regional and cellular patterns of Reelin mRNA expression in the forebrain of the developing and adult mouse. J. Neurosci. 18, 7779–7799 (1998).

76. C. Pesold, W. S. Liu, A. Guidotti, E. Costa, H. J. Caruncho, Cortical bitufted, horizontal, and Martinotti cells preferentially express and secrete Reelin into perineuronal nets, nonsynaptically modulating gene expression. Proc. Natl. Acad. Sci. U.S.A. 96, 3217–3222 (1999).

77. R. Feil, J. Wagner, D. Metzger, P. Chambon, Regulation of Cre recombinase activity by mutated estrogen receptor ligand-binding domains. Biochem. Biophys. Res. Commun. 237, 752–757 (1997).

78. National Research Council, Guide for the Care and Use of Laboratory Animals (National Academies Press, Washington, DC, ed. 8, 2011).

NEUROSCIENCE

Kim et al.
A key requirement for synaptic Reelin signaling in ketamine-mediated behavioral and synaptic action

PNAS | 11 of 11
https://doi.org/10.1073/pnas.2103079118